Baltic Astronomy, vol.1, 7–16, 1992.

SURFACE PHOTOMETRY OF GALAXIES. I. NGC 3379 AND M 81

Peeter Tenjes

Tartu Astrophysical Observatory, Tõravere 202444, Estonia

Received April 5, 1991.

Abstract. Two-dimensional photographic surface photometry has been derived for the standard elliptical galaxy NGC 3379 in the B-colour and for the spiral galaxy M 81 in the B- and U-colours. Galactic isophotes have been approximated by ellipses, and the major and minor axes profiles for the observed galaxies have been derived. The brightness profile in the EW-direction for NGC 3379 has been compared with the standard luminosity distribution of de Vaucouleurs and Capaccioli (1983). We find that our image processing system enables us to derive accurate results at least up to 1% from the sky level. Our results for the colour structure of M 81 indicate that the $U-B$ colour index of the galaxy becomes bluer outwards. Isophotes of the colour index are similar to the isophotes of the B surface brightness.

Key words: galaxies – surface photometry – structure of galaxies

1. Introduction

M 81 = NGC 3031, type Sa(s)ab, is a nearby galaxy suitable for detailed studies of the stellar content and for discrimination of stellar ensembles by their age, kinematics and spatial distribution. M 81 is often referred to as an example of galaxies with a falling rotational curve. In connection with this we have to answer an additional question, if there is any dark matter associated with M 81. To solve these problems, a detailed model for the distribution and chemical composition of the visible matter is needed first.

By now the surface photometry of M 81 exists in the B, V and R colours. The information on the light distribution in the U-band

is contradictory and scanty. At the same time the colour index $U-B$ is more informative than, e.g. the index $B-V$, if we study the chemical composition of galaxies. The purpose of the present paper is to derive the surface brightness profile of M 81 in the B- and U-colours along its minor and major axes.

The second galaxy, NGC 3379, has been selected by the Working Group on Galaxy Photometry of IAU Commission 28 (*IAU Trans.*, XIB, p.304) as a proper candidate for the establishment of luminosity distribution standards. It defines a 'standard' surface brightness distribution and detailed analysis of its surface photometry has been done by de Vaucouleurs and Capaccioli (1979). We use it to test our data processing algorithms.

2. Observations

The plate material consists of seven $5° \times 5°$photographs of different exposures in the B- and U-colours (Table 1) taken in March and August, 1983 with the Latvian 80/120/240 Schmidt telescope in Baldone. The plate scale is 85 $''$/mm.

Table 1. The plate material

Central object	Emulsion + filter	Colour system	Expos. time min	Seeing $''$
NGC 3379	ZU21+GG13	B	30	2-3
NGC 3379	ZU21+GG13	B	7	2-3
NGC 3031	ZU21+GG13	B	30	2-3
NGC 3031	ZU21+GG13	B	9	5
NGC 3031	ZU21+GG13	B	3	2-3
NGC 3031	ZU21+UG1	U	40	2
NGC 3031	ZU21+UG1	U	10	2

For calibration at the edges of every plate two sets of calibration spectrograms with different exposure times were made. Both sets provide 8 calibration bands, each with intensity ratios of about 1.4 between neighbouring bands.

The plates were digitized with a microdensitometer PDS 1010A at the Tõravere Observatory, and the density distributions $D(x, y)$ of the object galaxy and the surrounding area were recorded on a magnetic tape in the form of digital arrays of 500×500 pixels. The scanning was made with a square 20 μm diaphragm and with 20μm

stepping intervals for the plates of short exposures (less then 10^m) and with a 50 μm diaphragm and 50 μm stepping intervals for all other plates. The long-exposure plates were scanned also with a step of 100 μm to measure more blank sky areas. The calibration spectrograms were scanned with the same scanning parameters as the galaxies.

3. Data reduction

Digital frames were processed using the Tartu Image Data Analysis System, a set of software procedures that have been designed mainly for the surface photometry of galaxies. This system was initialized and developed by a working group from the Tõravere Observatory, which included the author of this paper. Some of the software has been published (Liiv, 1989), but the description of the whole system awaits publication yet.

In principle, the basic steps of the surface photometry of the galaxies are well known and presented in several papers (e.g. Jones et al., 1968; Barbon et al., 1976; Capaccioli, 1987; Okamura, 1988). However, there still exist large discrepancies between the results derived by various authors even in case of well-observed galaxies, e.g. M 87 (Carter and Dixon, 1978). For this reason we shall describe the processing in somewhat more detail.

At first, the initial data array needs to be filtered. For this purpose an adaptive filter is better than the common median-filters, gaussian smoothing or simple averaging procedures. This filter is desiged to increase the signal-to-noise ratio of digitized images and to reduce the redundancy in digital information. But its most important feature for the present application is that it smoothes the data in the noisy outskirts of galaxies without smearing out the inner regions and the stellar images, i.e. the dimensions of the smoothing window depend on the density gradients (Kaasik, 1991). In our case the largest smoothing window used was 13×13 pixels.

The next step is to convert the densities of the photographic emulsion into the flux intensities. A characteristic curve is defined for each plate by plotting the densities of the calibration spectrograms at the wavelength intervals 4100Å–4700Å and 3500Å–3800Å for the B and U plates, respectively, against their known relative intensities. Both spectrogram sets are used to increase the dynamical range and to reduce the errors of the characteristic curve. Every point in the

characteristic curve was obtained as a mean of about 200 pixels. For the density-intensity relation the analytical function proposed by de Vaucouleurs (1968) $\log I = a \log \omega + b$, is used. In this formula $\omega = 10^{D-D_0} - 1$, where D_0 is the fog density, a and b are free parameters. Afterwards, the density distributions $D(x, y)$ are converted into the intensity distributions $I_{G+S}(x, y)$, here G means the galaxy and S means the sky.

The third step is determination of the sky background. This is the most crucial step in surface photometry (Carter and Dixon, 1978; Capaccioli and de Vaucouleurs, 1983). For this purpose a mask frame is constructed at first, to exclude certain regions. The mask frame includes *(a)* all pixels, which deviate from the mean value of the whole frame by more than 0.5 σ, where σ is the standard deviation; *(b)* all pixels in the box (or boxes), the dimensions of which are given interactively. Part *(a)* of the mask excludes all sufficiently bright stars and the plate defects, our criterion of 0.5σ is rather strong. Part *(b)* excludes the faint outer parts of the galaxy and some other bad areas, if needed. Usually the mask frame includes about 5–10 per cent of all pixels. The program calculates then the sky background as a two-dimensional polynomial in x and y with the help of a least-square algorithm. At the first iteration all pixels which have not been excluded by the mask frame are taken into account. Following Jones et al. (1969), in subsequent iterations the points, which deviate from the average by more than 2.5 σ (in the second iteration) and by 1.0 σ (in all other iterations), are also excluded. The process stops when no significant change is found between two subsequent solutions. This process is then repeated, varying the order of the polynomial. Inspecting the final background isophotes and the moments of the distribution of our approximation, the final order of the background polynomial is chosen. The background local sky level $I_S(x, y)$ under the object galaxy is interpolated and subtracted from $I_{G+S}(x, y)$, leaving only $I_G(x, y)$, the intensity distribution of the galaxy. Because of the large dimensions of the galaxy in the plate (10 mm) and long exposure times, we assume that small time-scale fluctuations and small-scale spatial variations of the airglow are smeared out during the exposures. Therefore, we can hope that our two-dimensional polynomial represents adequately the background intensity of the sky.

In practice, $I_G(x, y)$ is expressed in units of the local sky intensity as $I_{rel}(x, y) = \{I_{G+S}(x, y) - I_S(x, y)\}/I_S(x, y)$, where I_{rel} is the relative intensity. By carefully modelling the nonuniform sky back-

ground and normalizing $I_G(x,y)$ by $I_S(x,y)$, we can correct, at least to the first-order approximation, the intensity distribution of the galaxy for the nonuniformity of the actual night-sky brightness and for the nonuniformity of the background density due to vignetting and/or photographic processing. To increase the dynamical range of the brightness profiles and to reduce accidental errors, the relative intensity distributions obtained from different plates are combined to yield the final relative intensity distribution.

Finally, the zero point of the relative intensity, i.e., the sky brightness, μ_{sky} in mag/arcsec^2, is determined on the basis of photoelectric measurements by Sandage et al. (1969).

Isophotes at equally spaced values of surface brightness are extracted from photographic images through a 4-point linear interpolation algorithm. Firstly, cluster analysis is used to separate the stars, defects and the galaxies. The remaining isophotes are approximated by ellipses. We assume that the galaxy is symmetric with respect to its center. A least square fitting algorithm finds five parameters: the semi-axis lengths a and b, the center coordinates (x_o, y_o) in the reference frame of the digital map and the azimuth of the major axis θ.

4. Results

In Fig. 1 comparison of our surface brightness data in the EW-direction for NGC 3379 with the results of de Vaucouleurs and Capaccioli (1979) is given. It is seen that our results do not deviate from the data now established as a standard by more than 0.2 mag even in the outer parts of the galaxy. The difference in the central $3''$ is due to the poorer resolution of our data. We find that our image processing system enables us to derive accurate results at least up to 1% from the sky level. For lower galactic brigtness levels a limiting restriction in the present case results from the calibration curve having too little number of points. This holds for both ends of the curve, to very high and very low density values.

The final light profiles for M 81 are presented in Table 2. Brightness is given in mag/arcsec^2 and the radii are in arcsec. A comparison with previous results is given in Figs. 2-4.

The existence of a colour gradient along the major axis is evident from Fig. 5. It may be the result of a combination of decreasing metallicity and decreasing mean age in the spheroidal and

Table 2. The observed surface brightness profiles of the galaxy M 81

B isophote	major axis	minor axis	*U* isophote	major axis	minor axis
18.68	12.4	8.7	19.37	11.1	8.14
18.85	15.6	10.3	19.45	13.2	9.13
19.15	20.6	14.0	19.50	15.9	10.1
19.40	27.8	19.3	19.58	18.4	11.8
19.48	31.2	21.8	19.68	19.6	12.7
19.83	41.6	28.6	19.75	22.4	15.2
20.20	55.2	32.5	19.85	24.3	18.7
20.45	64.5	41.4	19.95	27.9	22.3
20.60	71.8	45.1	20.55	41.6	33.2
20.75	77.9	50.9	20.65	47.1	35.0
20.85	81.8	56.8	20.73	51.5	36.5
21.05	102.9	72.0	20.83	55.5	38.2
21.15	110.5	76.2	20.90	61.5	40.1
21.35	127.5	79.6	21.00	66.0	43.6
21.50	153.	87.6	21.10	73.2	46.8
21.65	173.	91.8	21.18	75.6	50.3
21.85	202.	108.8	21.28	82.4	52.9
22.03	253.	133.5	21.35	84.6	59.2
22.15	303.	129.2	21.43	86.6	62.8
22.30	326.	145.	21.50	91.8	66.0
22.48	337.	185.	21.58	113.1	71.3
22.60	343.	200.	21.65	118.2	81.6
22.73	356.	209.	21.75	142.	87.6
22.90	371.	230.	21.85	159.	99.5
23.23	397.	259.	21.98	232.	101.2
23.35	423.	277.	22.10	275.	103.7
23.50	456.	278.	22.35	304.	186.
23.73	471.	298.	22.48	326.	187.
23.95	493.	317.	22.65	353.	200.
24.20	508.	414.	22.85	388.	250.
24.35	575.	421.	22.98	400.	249.
24.48	593.	430.	23.40	504.	314.

disk populations with increasing distance from the nucleus. In the inner regions of the galaxy, i.e. inside the bulge, the observed gradient is similar to those found in several other galaxies, e.g. M 31

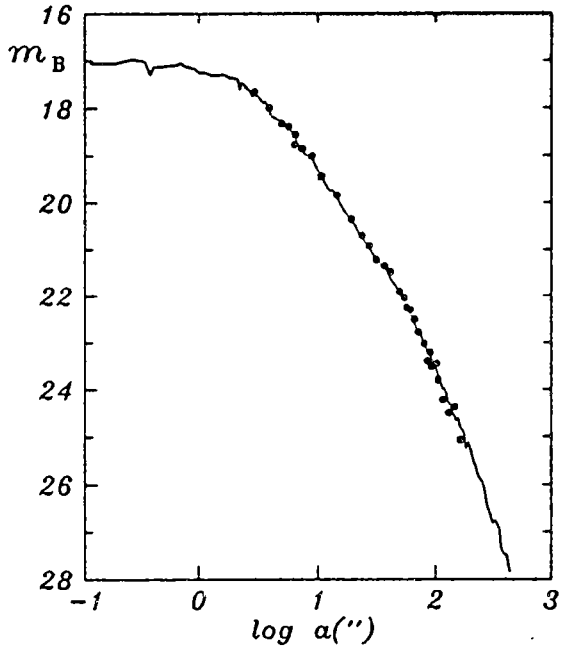

Fig. 1. The surface brightness of a standard elliptical galaxy NGC 3379. Solid line means the observations by de Vaucouleurs and Capaccioli (1979) and filled dots represent this work.

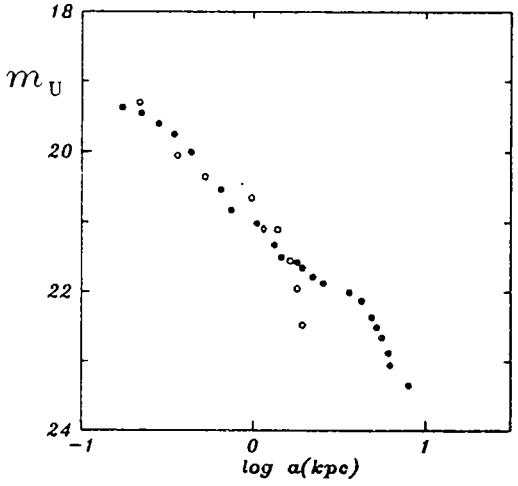

Fig. 2. The surface brightness of M 81 in the U-colour. Open circles are for Hoegner et al. (1971), diamond is for Sandage et al. (1969) and filled dots are for this work.

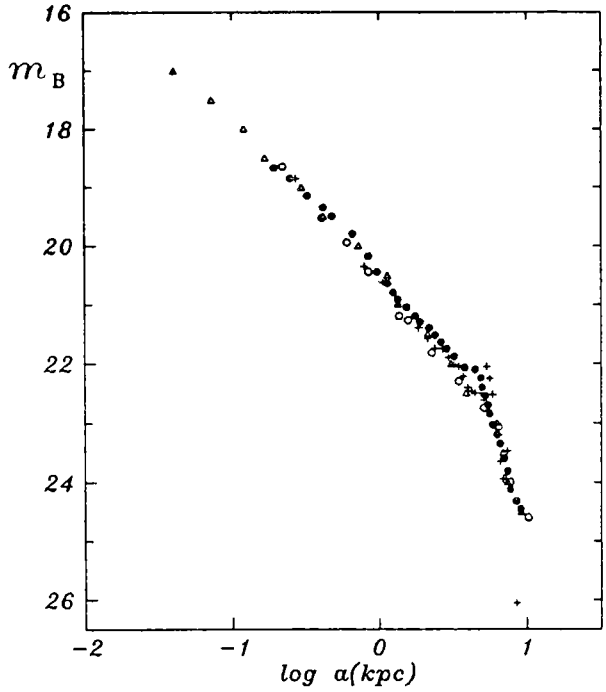

Fig. 3. The surface brightness of M 81 in the B-colour. Triangles are for Brandt et al. (1972), open circles are for Hoegner et al. (1971), crosses are for Markaryan et al. (1962) and filled dots are for this work.

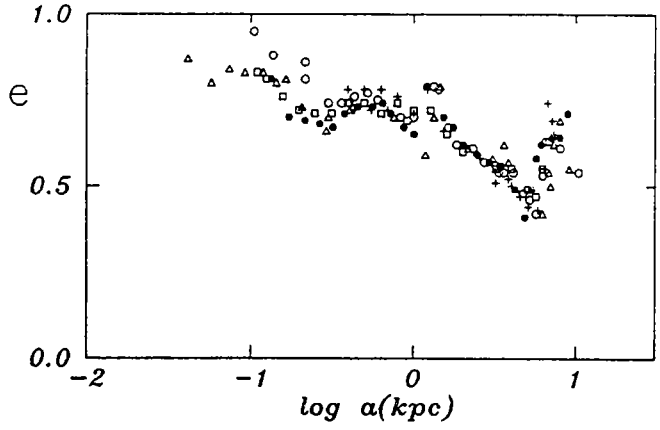

Fig. 4. The axial ratios e of the isophotes of M 81. Coded as in Figs. 2 and 3.

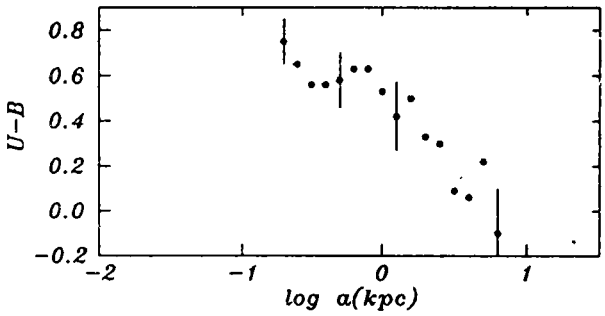

Fig. 5. The colour index $U-B$ of M 81.

(Sandage et al., 1969), M 51 (Okamura et al., 1976), etc. The increase of the metallicity in the inner regions of the bulges can be explained by the presence of a separate subsystem, a metal-rich core at the central region of the galaxy. Some other arguments supporting the core in case of M 31 were given by Tenjes et al. (1991). The decrease of the metallicity in the outer parts of M 81 is due to the presence of a population of young stars, i.e. the flat spiral-arm subsystem. This subsystem is seen also in Fig. 4, where a sharp decrease of the axial ratios is seen at the distance interval 3.5–5.5 kpc, the area rich in HII-regions (Hodge and Kennicutt, 1983). The detailed model of M 81 will be given as a subsequent paper in the series "Galactic models with massive coronae" published in *Astronomy and Astrophysics.*

Acknowledgments. Thanks are due to Director of the Latvian Radioastrophysical Observatory for the grant of the observing time, to Dr. A. Alksnis for his guidance in using the telescope and to Drs. M. Jõeveer and J. Vennik for their participation in the observations. I like to thank also the whole staff of the working group, especially, Drs. M. Liiv, A. Kaasik, E. Saar and I. Suisalu who actively participated in the developing of the Tartu Image Data Analysis System.

References

Barbon, R., Benacchio, L. and Capaccioli, M. 1976, Mem. Soc. Astron. Italiana, 47, 263.

Brandt, J.C., Kalinowski, J.K. and Roosen, R.G. 1972, ApJS, 24, 421.

Capaccioli, M. 1987, in Structure and Dynamics of Elliptical Galaxies, IAU Symp. No.127 (ed. T. de Zeeuw), Reidel, p. 47.
Capaccioli, M. and de Vaucouleurs, G. 1983, ApJS, 52, 465.
Carter, D. and Dixon, K.L. 1978, AJ, 83, 574.
de Vaucouleurs, G. 1968, Applied Optics, 7, 1513.
de Vaucouleurs, G. and Capaccioli, M. 1979, ApJS, 40, 699.
Hodge, P.W. and Kennicutt Jr., R.C. 1983, AJ, 88, 296.
Hoegner, W., Kadla, Z., Richter, N. and Strugatskaya, A. 1971, Astrofizika, 7, 407.
Jones, W.B., Gallet, R.M., Obitts, D. and de Vaucouleurs, G. 1967, Publ. Astron. Dept. Univ. Texas, Ser. 2, 1, No.8.
Kaasik, A. 1991, in preparation.
Liiv, M. 1989, Tartu Obs. Preprint A-6.
Markaryan, B.E., Oganesyan, E.Y. and Arakelyan, S.N. 1962, Soobshch. Byurakan Obs. No. 30, 3.
Okamura, S. 1988, PASP, 100, 524.
Sandage, A.R., Becklin, E.E. and Neugebauer, G. 1969, ApJ, 157, 55.
Tenjes, P., Haud, U. and Einasto, J. 1991, A&A, in press.